16th World Conference on Earthquake, 16WCEE 2017
Santiago Chile, January 9th to 13th 2017
Paper N° 3150 (Abstract ID)
Registration Code: S-H1463038961

DYNAMIC BEHAVIOR OF WOODEN BUILDING STRUCTURES INVOLVING STIFF CORES

Y. Yamazaki(1), H. Sakata(2)

(1) *Assistant Professor, Tokyo Institute of Technology, yamazaki.y.ai@m.titech.ac.jp*
(2) *Professor, Tokyo Institute of Technology, sakata.h.aa@m.titech.ac.jp*

Abstract

In Japan, construction of wood structures for public buildings is encouraged for environmental reason. For example, low-rise large wood buildings sometimes involve RC cores to enhance the seismic performance and the fire resistance. However, it is difficult to evaluate seismic force distribution and stress between wood parts and core parts of such horizontal hybrid structures. In this paper, applicability of simplified modeling method by two-dimensional continuous model to simulate the unique vibration properties of horizontal hybrid structures is discussed. Based on the theoretical approach, practical formulae of amplitude and distribution of seismic force acting on wood parts are proposed. The accuracy is demonstrated by comparison with earthquake response analyses.

Keywords: wooden structure, seismic force distribution, continuous model, response spectrum method, horizontal hybrid structure

1. Introduction

In Japan, wooden buildings have been mainly built as small detached houses so far. However, construction of wood structures for public buildings is encouraged for environmental reason. Low-rise large wood buildings sometimes involve RC cores to enhance the seismic performance and the fire resistance as shown in Fig. (1). Some experimental studies on wooden horizontal hybrid structure involving RC core or steel core have been reported, and the advantages in seismic resistance has been demonstrated through shaking table test [1, 2].
A prototype of such wooden horizontal hybrid structure was presented by Architectural Institute of Japan in 2012 [3]. Through the seismic design procedure of the prototype, it was revealed that the evaluation of seismic force distribution and the stress of connections between wood parts and core parts is quite difficult. Since the current design handbook for wooden hybrid structures does not treat the issues, time history analysis is required to determine the appropriate seismic force distribution. It is not suitable situation to promote constructions of large wooden buildings. Therefore, the objective of this research is to propose simplified design method of such horizontal hybrid structures with less effort.

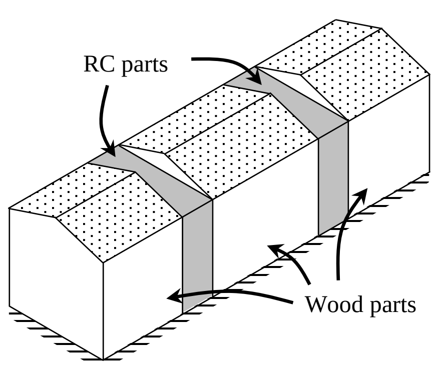

Fig. 1 – An example of horizontal hybrid structure of wood and RC

2. Basic vibration property of horizontal hybrid structure

2.1 Example building

Architectural Institute of Japan provided a prototype of hybrid structures of wood and RC in order to show the procedure of structural design [3]. Fig. 2 is the typical floor plan. It intends three-story school building having RC core parts from X4 to X5 and from X11 to X12.

Wood parts consist of glued-laminated timber's framing and plywood sheathing walls and floor diaphragms. Connections between timber beams and RC parts have only axial and shear resistance because it is generally difficult to realize moment resisting joints by wooden connections. Therefore moment of floor diaphragms must be resisted by a couple of axial forces of timber beams, and especially tensile force of timber beams should be precisely evaluated. RC cores are located in stair halls, and their structure is moment resisting frame with shear walls.

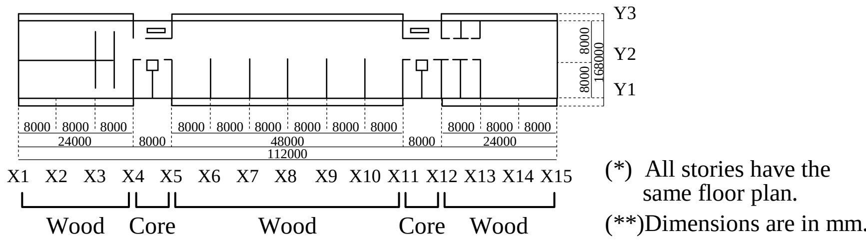

Fig. 2 – Floor plan of prototype building

2.2 Eigen value analysis

Eigen value analysis is carried out using lumped mass-shear spring model as shown in Fig. 3. Shear walls and floor diaphragms of wood parts are modeled by vertical and horizontal shear springs, respectively. RC parts are similarly modeled. The effect of torsion is supposed to be negligible. Properties of each element are shown in Table 1. Total weight of wood parts and RC parts are 12,653kN and 18,436kN, respectively.

The characteristics of important vibration modes are discussed here. Although total forty five modes can be obtained, two pairs of "wood part dominant modes" and "core part dominant modes" are focused on. Fig. 4(a) and (b) show wood part dominant 1st and 2nd modes, and Fig. 4(c) and (d) show core part dominant 1st and 2nd modes. Since the model is symmetric, Fig. 4 illustrates superposition of participation vectors of a few modes based on the modal shapes' and the natural periods' similarity. It was found that wood parts and core parts do not act in the same modes. Additionally, natural periods of wood and core part dominant modes are quite different. Therefore, these modes are not likely to be coupled.

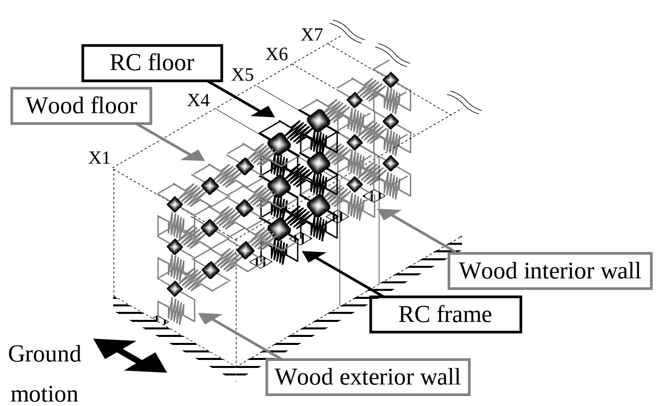

Fig. 3 – Vibration analysis model

Table 1 – Stiffness of shear springs (Unit: kN/cm)

	Wood		Core	
Lateral spring	Floor	135	Floor	28200
Vertical spring	Interior wall (X6～X10)	97.2	3F frame	27430
	Exterior wall (X1, X15)	256.2	2F frame	40550
			1F frame	54170

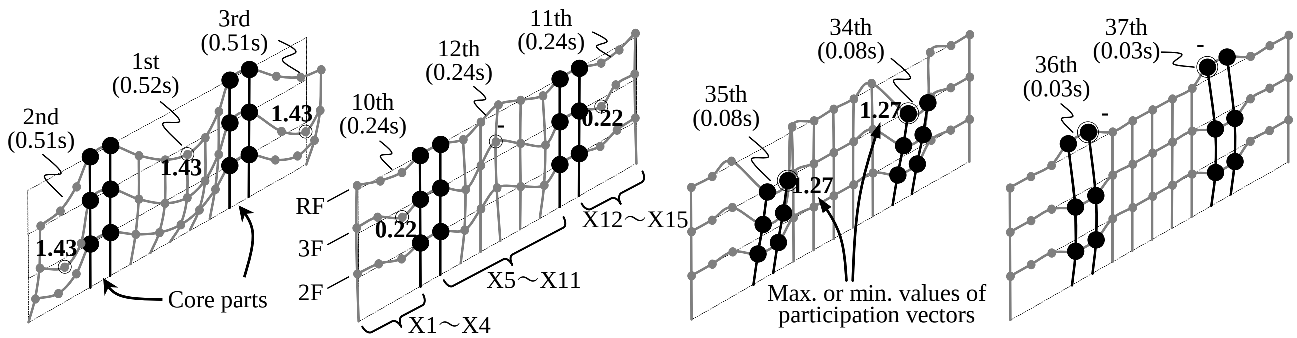

(a) Wood part dominant 1st mode (b) Wood part dominant 2nd mode (c) Core part dominant 1st mode (d) Core part dominant 2nd mode

Fig. 4 – Dominant participation vectors and natural periods

3. Modeling method by continuous body

Based on the discussion in the last chapter, core parts are unlikely to contribute to wood parts' response. Therefore core parts are assumed to be infinitely rigid when calculating wood parts' response.

If shear walls are distributed at small intervals like X5 to X11 (Fig. 2), they are able to be modeled by continuous shear springs. Therefore, the structure is idealized by uniform shear panel considering its out of plane deformation having different shear moduli in two directions as shown in Fig. 5. In practical designs, shear walls may be concentrated on outer frame like X1 to X4 (Fig. 2). Such structures, however, are not treated in this research.

3.1 Modeling by uniform shear panel and the dominant equation

Equilibrium of forces in infinitesimal portion of uniform shear panel is expressed as shown in Fig. 6. Displacement u satisfies the following partial differential equation whose parameters are two-dimensional coordinates(x and y) and time(t).

$$\rho \frac{\partial^2 u}{\partial t^2} = G_x \frac{\partial^2 u}{\partial x^2} + G_y \frac{\partial^2 u}{\partial y^2} \tag{1}$$

Where, ρ = specific gravity of the body, G_x, G_y = shear moduli in x- and y-direction, respectively. G_x and G_y represent the stiffness of floor diaphragm and shear wall, respectively, and they are expressed as follows.

$$G_x = l_f \sum_y k_f \Big/ \left(H - h/2\right) \ , \ \ G_y = h \sum_x k_w \Big/ \left(L_f - l_f/2\right) \tag{2a,b}$$

Where, k_f is shear stiffness of floor diaphragm in unit span (l_f). k_w is shear stiffness of shear wall in unit story height (h). L_f and H are building width and height, respectively.

Eq.(1) is a kind of equation of wave motion. However, the body has anisotropy. In order to simulate one-side core, the following boundary conditions are given.

$$u(0,y,t)=0\ ,\ \ u(x,0,t)=0 \tag{3a,b}$$

$$\frac{\partial u(L_f\,,y,t)}{\partial x}=0\ ,\ \ \frac{\partial u(x,H,t)}{\partial y}=0 \tag{4a,b}$$

In the case of $G_x/L_f^2 = G_y/H^2$, the model can be called "isotropic uniform shear panel" because it shows symmetric behavior in two diagonal directions. If the condition is not satisfied($G_x/L_f^2 \neq G_y/H^2$), it can be called "anisotropic uniform shear panel".

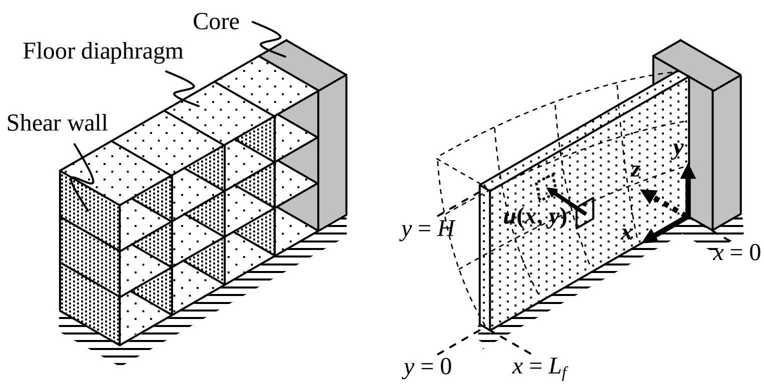

(a) Original model (b) Uniform shear panel

Fig. 5 – Modeling method by continuous body

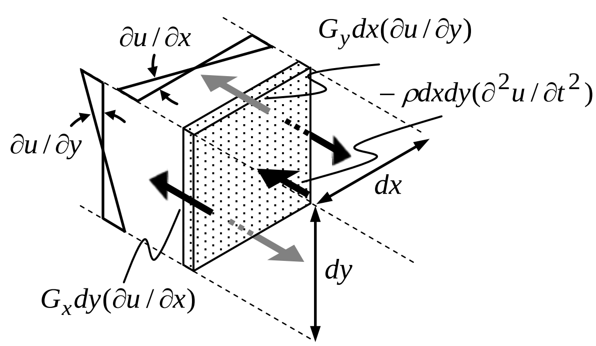

Fig. 6 – Equilibrium of forces in infinitesimal portion of uniform shear panel

3.2 Modal properties

The eigen value problem of Eq. (1) can be solved by using variable separation. The following is the eigen function $\phi_{mn}(x, y)$.

$$\phi_{mn}(x,y)=\sin\frac{(2m-1)\pi x}{2L_f}\sin\frac{(2n-1)\pi y}{2H} \tag{5}$$

Where, m and n are mode numbers of eigen function in x- and y- direction, respectively. Corresponding natural circular frequency and participation factor of (m, n)th mode ω_{mn}, β_{mn} are expressed as follows.

$$\omega_{mn} = \sqrt{\left(\frac{(2m-1)\pi}{2L_f}\right)^2 \frac{G_x}{\rho} + \left(\frac{(2n-1)\pi}{2H}\right)^2 \frac{G_y}{\rho}} \tag{6}$$

$$\beta_{mn} = \frac{\int_0^H \int_0^{L_f} \phi_{mn}(x,y)dxdy}{\int_0^H \int_0^{L_f} (\phi_{mn}(x,y))^2 dxdy} = \frac{16}{\pi^2 (2m-1)(2n-1)} \tag{7}$$

Seismic force acting above *i*-th floor caused by (m, n)th mode $Q_{i,mn}$ is as follows.

$$\begin{aligned} Q_{i,mn} &= S_{pa,mn} \rho \int_{y_i}^H \int_0^{L_f} \beta_{mn} \phi_{mn}(x,y)dxdy \\ &= \frac{S_{pa,mn} W}{g} \frac{64}{\pi^4 (2m-1)^2 (2n-1)^2} \cos\frac{(2n-1)\pi y_i}{2H} \end{aligned} \tag{8}$$

Where, $S_{pa,mn}$ is pseudo acceleration spectrum of (m, n)th mode, y_i is height at *i*-th floor, W is total weight of wood part (= $\rho g L_f H$) and g is gravity acceleration, respectively. Since the force is resisted not only by wood part but by core part, $Q_{i,mn}$ consists of shear force of shear walls in *i*-th story and shear force of floor diaphragms above *i*-th floor.

4. Formulation of seismic force distribution

4.1 Spectrum method

In the following expressions, x and y can be clearly relaced, which means not only vertical distribution but lateral distribution of seismic force are able to be derived by the same procedure. In this paper, the vertical distribtuion is focused on.

In the beginning, the shape of pseudo acceleration spectrum is modeled. Similar to the general tendency, constant acceleration for short period structures and constant velocity for long period structures are considered. As a result, the following expressions are obtained.

$$\omega_{mn} = \omega_x \sqrt{(2m-1)^2 + \beta(2n-1)^2} \;\;,\;\; \beta = \frac{\omega_y^2}{\omega_x^2} = \frac{G_y L_f^2}{G_x H^2} \tag{9a,b}$$

$$\omega_x = \sqrt{\left(\frac{\pi}{2L_f}\right)^2 \frac{G_x}{\rho}} \;\;,\;\; \omega_y = \sqrt{\left(\frac{\pi}{2H}\right)^2 \frac{G_y}{\rho}} \tag{10a,b}$$

$$S_{pa,mn} = S_{pa1} \left(\frac{\omega_{mn}}{\omega_{11}}\right)^k = S_{pa1} \left(\frac{(2m-1)^2 + \beta(2n-1)^2}{1+\beta}\right)^{k/2} \tag{11a,b}$$

Where, S_{pa1} is pseudo acceleration spectrum of fundamental mode. k = 0 and 1 represent constant acceleration and constant velocity, respectively. $\beta = G_x/L_f^2 = G_y/H^2$ is named anisotropic parameter because β = 1 means isotropic uniform shear panel.

4.2 Degeneracy

Fig. 7 shows list of eigen function of (m, n)th mode. They are common for isotropic and anisotropic uniform shear panel. However, in the case of isotropic uniform shear panel, natural circular frequency of (m, n)th mode and (n, m)th mode are clearly the same, which results in degeneracy modes. Two modes in diagonal positions in

Fig. 7 are degeneracy relation. Although SRSS (Square-Root of Sum of Squares) method is generally used to combine modal responses, simple sum have to be applied for degeneracy modes. Note that such relations can be observed not only between (m, n)th mode and (n, m)th mode but between (5, 4)th and (6, 2)th and so on. In this research, degeneracy between (m, n)th mode and (n, m)th mode is considered.

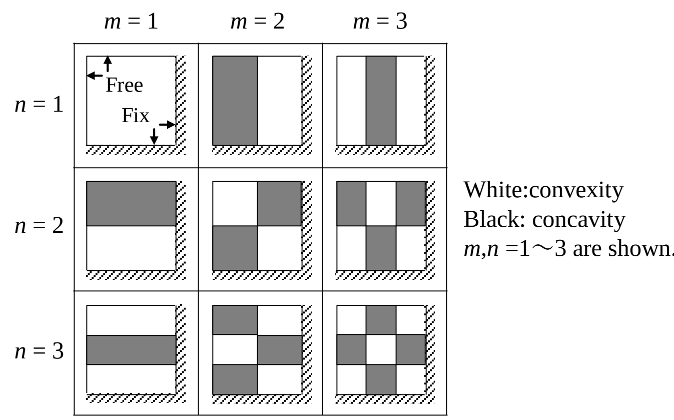

Fig. 7 – List of eigen function of (m, n)th mode

4.3 Seismic force distribution of isotropic uniform shear panel

As mentioned above, $Q_{i,mn}$ is combined using simple sum between (m, n)th mode and (n, m)th mode and SRSS method for others as follows.

$$
\begin{aligned}
Q_i &= \sqrt{\sum_{m=1}^{\infty}(Q_{i,mm})^2 + \sum_{m=1}^{\infty}\sum_{n=m+1}^{\infty}(Q_{i,mn}+Q_{i,nm})^2} \\
&= \sqrt{\sum_{m=1}^{\infty}\sum_{n=1}^{\infty}(Q_{i,mn})^2 + \sum_{m=1}^{\infty}\sum_{n=1}^{\infty}Q_{i,mn}Q_{i,nm} - \sum_{m=1}^{\infty}(Q_{i,mm})^2}
\end{aligned}
\tag{12}
$$

$$
\sum_{m=1}^{\infty}\sum_{n=1}^{\infty}(Q_{i,mn})^2 = \left(\frac{64S_{pa1}W}{\pi^4 g}\right)^2 \sum_{m=1}^{\infty}\sum_{n=1}^{\infty}\frac{\left[\frac{(2m-1)^2+(2n-1)^2}{2}\right]^k}{(2m-1)^4(2n-1)^4}\cos^2\frac{(2n-1)\pi y_i}{2H}
$$

$$
\sum_{m=1}^{\infty}\sum_{n=1}^{\infty}Q_{i,mn}Q_{i,nm} = \left(\frac{64S_{pa1}W}{\pi^4 g}\right)^2 \sum_{m=1}^{\infty}\sum_{n=1}^{\infty}\frac{\left[\frac{(2m-1)^2+(2n-1)^2}{2}\right]^k}{(2m-1)^4(2n-1)^4}\cos\frac{(2m-1)\pi y_i}{2H}\cos\frac{(2n-1)\pi y_i}{2H}
\tag{13a-c}
$$

$$
\sum_{m=1}^{\infty}\left(Q_{i,mm}\right)^2 = \left(\frac{64S_{pa1}W}{\pi^4 g}\right)^2 \sum_{m=1}^{\infty}\frac{\left[(2m-1)^2\right]^k}{(2m-1)^8}\cos^2\frac{(2m-1)\pi y_i}{2H}
$$

Infinite series in Eq. (13) are calculated as follows.

1) In the case of constant acceleration spectrum (k = 0)

$$
\sum_{m=1}^{\infty}\sum_{n=1}^{\infty}(Q_{i,mn})^2 = \left(\frac{64S_{pa1}W}{g}\right)^2 \frac{1}{9216}\left(1-3Y_i^2+2Y_i^3\right)
$$

$$\sum_{m=1}^{\infty}\sum_{n=1}^{\infty}Q_{i,mn}Q_{i,nm} = \left(\frac{64S_{pa1}W}{g}\right)^2 \frac{1}{9216}\left(1-\frac{3}{2}Y_i^2+\frac{1}{2}Y_i^3\right)^2 \tag{14a-c}$$

$$\sum_{m=1}^{\infty}\left(Q_{i,mm}\right)^2 = \left(\frac{64S_{pa1}W}{g}\right)^2 \frac{1}{322560}\left(34-84Y_i^2+70Y_i^4-28Y_i^6+8Y_i^7\right)$$

The following variable transformation was used.

$$Y_i = y_i / H \tag{15}$$

2) In the case of constant velocity spectrum (k = 1)

$$\sum_{m=1}^{\infty}\sum_{n=1}^{\infty}(Q_{i,mn})^2 = \left(\frac{64S_{pa1}W}{\pi g}\right)^2 \frac{1}{1536}\left[\left(1-3Y_i^2+2Y_i^3\right)+(1-Y_i)\right]$$

$$\sum_{m=1}^{\infty}\sum_{n=1}^{\infty}Q_{i,mn}Q_{i,nm} = \left(\frac{64S_{pa1}W}{\pi g}\right)^2 \frac{1}{768}(1-Y_i)\left(1-\frac{3}{2}Y_i^2+\frac{1}{2}Y_i^3\right) \tag{16a-c}$$

$$\sum_{m=1}^{\infty}\left(Q_{i,mm}\right)^2 = \left(\frac{64S_{pa1}W}{\pi g}\right)^2 \frac{1}{1920}\left(2-5Y_i^2+5Y_i^4-2Y_i^5\right)$$

4.4 Seismic force distribution of anisotropic uniform shear panel

Assuming that there are no degeneracy modes, all modes are combined by SRSS method as follows.

$$Q_i = \sqrt{\sum_{m=1}^{\infty}\sum_{n=1}^{\infty}(Q_{i,mn})^2} = \frac{64S_{pa1}W}{\pi^4 g}\sqrt{\sum_{m=1}^{\infty}\sum_{n=1}^{\infty}\frac{\left[\frac{(2m-1)^2+\beta(2n-1)^2}{1+\beta}\right]^k}{(2m-1)^4(2n-1)^4}\cos^2\frac{(2n-1)\pi y_i}{2H}} \tag{17}$$

In the case of constant velocity spectrum (k = 1), the closed-form solution is not obtained in the above equation. Therefore numerical solution is shown for discussion later. The solution for k = 0 is introduced below.

$$Q_i = \frac{64S_{pa1}W}{g}\frac{\sqrt{1-3Y_i^2+2Y_i^3}}{96} \tag{18}$$

4.5 Base shear coefficient

By substituting Y_i = 0 into various Q_i, tendency of base shear force Q_1 is discussed. Note that the base shear force is derived from seismic force acting on wood part. In other words, the seismic force acting on core part is omitted.

In the case of isotropic uniform shear panel,

$$Q_1\big|_{k=0} = 0.676Q_{SDOF} \;,\quad Q_1\big|_{k=1} = 0.805Q_{SDOF} \tag{19a,b}$$

In the case of anisotropic uniform shear panel,

$$Q_1\big|_{k=0} = 0.667Q_{SDOF} \;,\quad Q_1\big|_{k=1} = 0.731Q_{SDOF} \tag{20a,b}$$

Where, Q_{SDOF} is $S_{pa1}W/g$. The factor multiplied by Q_{SDOF} represents reduction ratio of base shear force compared to SDOF system having the same weight and fundamental period. According to the theory for one-dimensional continuous shear bar model, the factor is 0.816 for constant acceleration spectrum and 0.9 for constant velocity spectrum, respectively as stated by Ishiyama [4]. Therefore the reduction ratio is likely to be smaller in two-dimensional model like horizontal hybrid structure.

5. Application to discretized model

In this section, a method to apply the theoretical solution for continuous model to discretized model like lumped mass-shear spring model.

5.1 Base shear coefficient in wood part

As mentioned before, the base shear force derived in section 4.5 considers seismic force acting on wood part. Therefore it is called base shear force in wood part, and the one divided by total weight of wood part is called base shear coefficient in wood part.

Because horizontal hybrid structures are likely to be introduced in low-rise building, the vibration model is developed by lumped mass-shear spring model with small number of nodes as shown in Fig. 3. When applying the theoretical solution for continuous model to such discretized model, non-negligible error may arise. For example, if a structure is single story and single span, base shear coefficient in wood part is clearly $Q_1 = Q_{SDOF}$ unlike Eq. (19) and (20). It can be recognized as effect of equivalent mass ratio of 1st mode. Therefore the tendency of base shear coefficient in wood part with respect to the number of stories and spans are investigated.

Fig. 8 shows lumped mass-shear spring model with M-span and N-story representing a model whose mass and stiffness are equally distributed. Seven cases of M (= N= 1, 2, 3, 5, 12, 20), three cases of β (= 0.67, 1, 1.5, Eq. (9b)) and two cases of natural period of 1st mode T_1 (= 0.5, 1.5 sec) are considered. Total 42 cases of earthquake response analyses are carried out. Four artificial earthquakes having a phase property of Elcentro-NS, Taft-EW, Hachinohe-NS and JMA Kobe-NS earthquake are generated [5]. Target response spectra of the input motions are shown in Fig. 9. It has constant pseudo acceleration region from 0.16 to 0.6 second, and the intensity is 0.2 times of gravity acceleration.

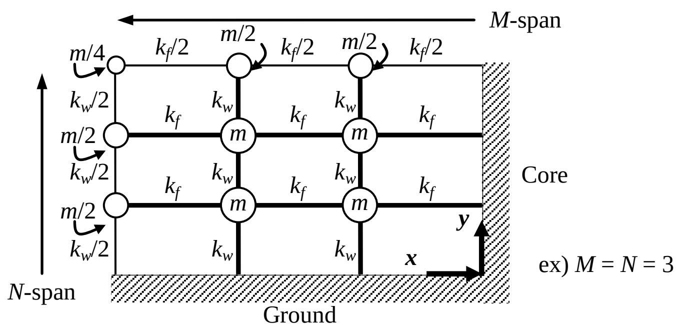

Fig. 8 – Discretized model of uniform shear panel considering M x N DOF

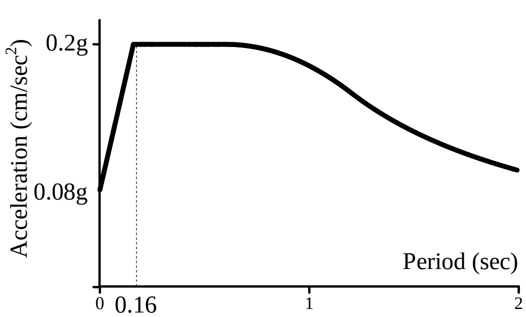

Fig. 9 – Target pseudo acceleration spectrum of input motions

Fig. 10 shows the tendency of base shear coefficient in wood part with respect to M (= N). Averaged results of four input motions are indicated. In the case of M = 1, the base shear coefficient in wood part corresponds to $S_{pa}(T_1)$ divided by g. However, the base shear coefficient in wood part is approaching theoretical solution for continuous model (= $0.67S_{pa}(T_1)/g$) as M becomes large. Since the base shear coefficient in wood part is not so reduced as the theoretical solution even in M = 20, the tendency in Fig. 10 have to be referred to estimate the base shear coefficient according to the number of stories and spans. In this case, $Q_1 = 0.9Q_{SDOF}$ seems appropriate because $M = N = 3$ is considered.

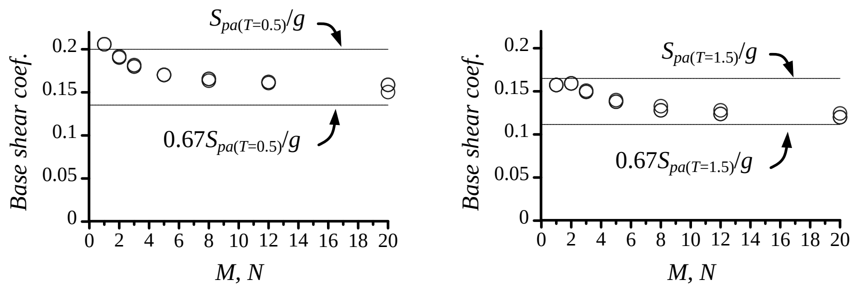

(*) Averaged result of four motions, β = 0.67, 1, 1.5 are shown.

(a) T_1 = 0.5sec (b) T_1 = 1.5sec

Fig. 10 – Base shear coefficient in wood part obtained by earthquake response analyses

5.2 Seismic vertical shear coefficient distribution in wood part

In this paper, seismic vertical shear coefficient distribution A_i is defined as seismic force acting above i-th floor Q_i divided by weight above i-th floor [4]. A_i is normalized by A_1 (i. e. A_1 = 1). In the following discussion, constant acceleration spectrum is considered because most of horizontal hybrid structures are introduced in low-rise building. Since A_i of isotropic and anisotropic uniform shear panel are almost same in constant acceleration region [6], the solution for anisotropic uniform shear panel is used. Based on definition in Japanese code, parameter Y_i is replaced by normalized weight α_i, and the formula is expressed as follows.

$$A_i = \sqrt{(3-2\alpha_i)}\ , \quad \alpha_i = \sum_{j=i}^{N} W_j \Bigg/ \sum_{j=1}^{N} W_j \tag{21a,b}$$

Where, α_i is normalized weight of i-th floor, W_j is weight of j-th floor and N is the number of floor, respectively. The expression is the same as the one of theoretical solution for uniform shear bar [4]. However, since Eq. (21) is not appropriate to be applied to discretized model, the following modification is proposed.

In order to deal with non-uniform distribution of mass and stiffness, normalized weight α_i in Eq. (21b) is modified as follows.

$$\alpha_i' = \begin{cases} \left(\sum_{j=i}^{N-1} W_j + W_N R_N\right) \Bigg/ \left(\sum_{j=1}^{N-1} W_j + W_N R_N + 0.5W_1\right) & (i \neq N) \\ \left(W_N R_N\right) \Bigg/ \left(\sum_{j=1}^{N-1} W_j + W_N R_N + 0.5W_1\right) & (i = N) \end{cases} \tag{22}$$

$$R_N = \left(\sqrt{\frac{k_{f,N-1}/W_{N-1}}{k_{f,N}/W_N}\cdot\beta} + 1\right) \Bigg/ \left(\sqrt{\beta} + 1\right) \tag{23}$$

Where, R_N is modification factor to be multiplied by W_N. The theory originally intends model illustrated in Fig. 8 regarding distribution of mass and stiffness. However, it is not always satisfied in actual building. Particularly shear stiffness of floor diaphragm at top floor is usually the same as the ones of other floors. The error caused by it tries to be minimized by R_N. In addition, $0.5W_1$ in denominator of right member of Eq. (22)

contributes to modification. Weight of lower half of 1st story is not included in seismic force while continuous model clearly includes it. As a result, modified A'_i is expressed as follows.

$$A'_i == \frac{1}{\alpha_i}\frac{\alpha'_i}{\alpha'_1}\sqrt{\frac{3-2\alpha'_i}{3-2\alpha'_1}} \tag{24}$$

The adequacy of the modification is discussed using one-dimensional model for simplification. Fig. 11(a) shows N-story lumped mass-shear spring model. N = 2, 3, 5, 8, 12, 20 are considered. Fig. 11(b) shows comparison of seismic vertical shear coefficient distribution obtained by A_i (Eq. (21a)), A'_i (Eq. (24), R_N = 1) and numerical analysis result using SRSS method. A'_i is close to SRSS at all stories while A_i is overestimated at upper story. The larger N is, the less the error of A_i is. However, A'_i is clearly effective especially for low-rise building. The adequacy of R_N is discussed in the next chapter, which is not mentioned here.

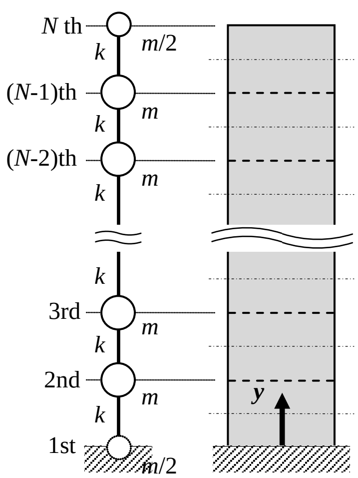

(a) Model

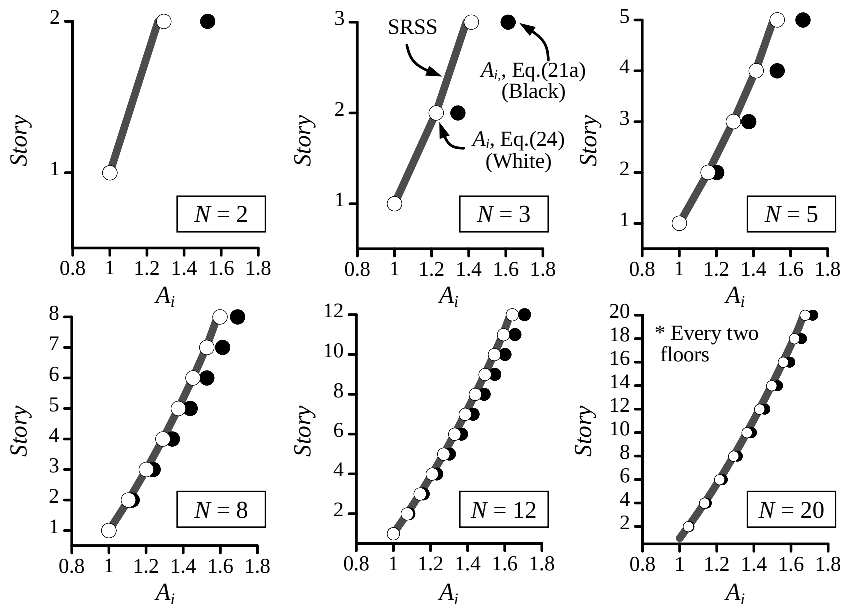

(b) Comparison of seismic vertical shear coefficient distribution

Fig. 11 – Adequacy of modification for discretized model

6. Verification of applicability by numerical analysis

6.1 Analysis model

Earthquake response analysis is conducted using the vibration model as shown in Fig. 3, and behavior of the model from X5 to X11 is compared. All spring elements are elastic. Damping matrix of the model is constructed so that damping ratio of all vibration modes become 5%. The model having the properties shown in Table 1 is named "basic model" which is the prototype provided by AIJ. In addition, models having various stiffness of wooden shear walls and floor diaphragm as shown in Table 2 are analyzed. "Mass" model and "Stiffness" model whose R_N is 1.0 are also considered to discuss the adequacy of R_N proposed in the last chapter.

6.2 Natural period

Table 3 shows comparison of natural period of 1st mode between eigen value analysis result (analysis) and theoretical solution (evaluation, Eq. (6)). Although evaluation is about 10% shorter than analysis, tendency with respect to stiffness balance can be simulated.

6.3 Base shear coefficient in wood part

Table 4 shows base shear coefficient in wood part obtained by earthquake response analyses. Averaged results of four input motions are indicated. Values in parentheses are normalized by 0.2 which is the base shear coefficient of SDOF. They are from 0.9 to 0.95 as is expected from the tendency in Fig. 10.

Table 2 – List of models

	Name	Property	β
1	Basic	Model having the properties of prototype[2)] (Table1)	0.6
2	Floor*0.5	Stiffness of floor diaphragms are half.	1.2
3	Floor*2.0	Stiffness of floor diaphragms are twice.	0.3
4	Wall*0.5	Stiffness of shear walls are half.	0.3
5	Wall*2.0	Stiffness of shear walls are twice.	1.2
6	Mass	Mass of the top story are twice.	0.6
7	Stiffness	Stiffness of floor diaphragm of the top story is half.	0.72

Table 3 –Natural period of 1st mode

	Basic	Floor*0.5	Floor*2.0	Wall*0.5	Wall*2.0
Analysis	0.52	0.63	0.41	0.58	0.45
Evaluation	0.48	0.58	0.38	0.54	0.41

Unit:second

Table 4 – Seismic force acting on wood part

	Basic	Floor*0.5	Floor*2.0	Wall*0.5	Wall*2.0
Analysis	0.189 (0.94)	0.180 (0.90)	0.187 (0.94)	0.188 (0.94)	0.189 (0.95)

Normalized by weight of wood part
(Normalized by base shear force of SDOF)

Non-dimensional

6.4 Seismic vertical shear coefficient distribution in wood part

Fig. 12 shows comparison of seismic vertical shear coefficient distribution in wood part which is expressed as C_i (= C_0A_i). C_0 is base shear coefficient in wood part, and C_0 = 0.2 x 0.9 is considered based on the numerical analysis results mentioned in section 5.1 and 6.3. C_i (= C_0A_i), C'_i (= $C_0A'_i$) and $C_{i,ana}$ (earthquake response analysis result) are compared. "Wall*0.5" and "Wall*2.0" are omitted because they are almost same as "Floor*2.0" and "Floor*0.5", respectively. C'_i approximately corresponds to average of $C_{i,ana}$ while C_i is overestimated at upper story. In addition, $C_{i,ana}$ of "Mass" and "Stiffness" show liner distribution, and C'_i can simulate such tendency.

7. Conclusions

The followings are findings of this paper.

1) Dynamic behavior of horizontal hybrid structure provided by AIJ was analyzed. Since wood parts and core parts had quite different vibration properties, they did not act in the same vibration modes.

2) Simplified modeling method of horizontal hybrid structure were presented. If shear walls are distributed at small intervals, idealized uniform shear panel considering its out of plane deformation having different shear stiffness in two directions was applied.

3) Based on the model, practical formulae of fundamental period, amplitude and distribution of seismic force

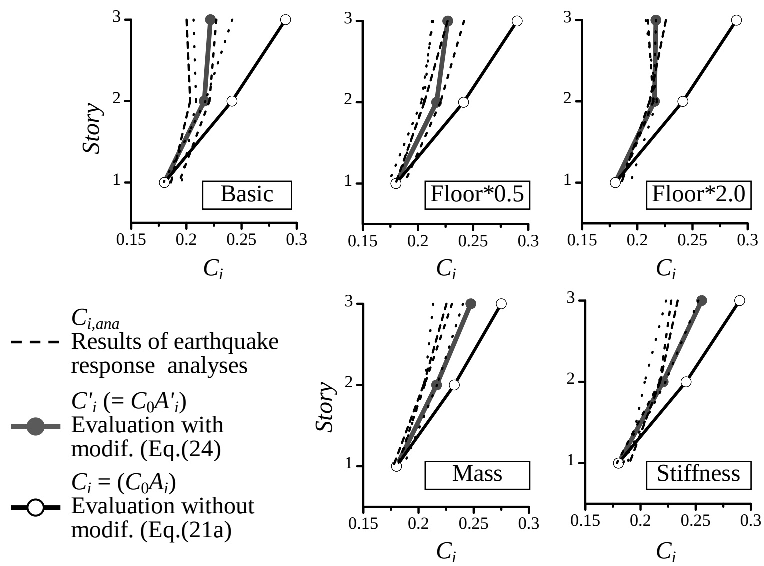

Fig. 12 – Comparison of seismic vertical shear coefficient distribution in wood part of various models

acting on wood parts were derived. A technique to apply the theoretical solution for continuous model to discretized model like lumped mass-shear spring model was also proposed.

4) The accuracy of the formulae was demonstrated by comparison with earthquake response analyses, and they gave close agreement.

Acknowledgements

This work was supported by JSPS KAKENHI Grant Number JP26709039.

References

[1] Isoda H, Kawai N, Koshihara M, Araki Y, Tesfamariam S (2016): Timber–reinforced concrete core hybrid system: Shake table experimental test, *Journal of Structural Engineering*, ASCE, 10.1061/(ASCE)ST.1943-541X.0001631, 04016152

[2] Kawai N, Isoda H, Koshihara M, Minowa C, Araki Y (2006): Shaking table tests on scaled models of timber-based hybrid structure(in Japanese), *Summaries of technical papers of annual meeting 2006*, Architectural Institute of Japan, **C-1**, 169-170

[3] Architectural Institute of Japan (2012): Daikibomokuzoukenchikuno gijutsutekikadaito kaiketsuhoho(in Japanese), *Material of AIJ annual meeting*

[4] Ishiyama Y (1988): Proposal for A distribution of seismic shear coefficient along the height of a building, *Proceedings of 9th World Conference on Earthquake Engineering*, 977-982

[5] Sada T, Hiramatsu G, Hasegawa Y, Sakata H, Kasai K (2012): Development of passively-controlled houses with superior property-retention capability: Part 40 Recommendation of input earthquake motion for seismic design of passively-controlled houses(in Japanese), *Summaries of technical papers of annual meeting 2012*, Architectural Institute of Japan, **B-2**, 1001-1002

[6] Yamazaki Y, Sakata H (2016): Simplified modeling method and Seismic force evaluation of building structures involving stiff cores: Study on dynamic behavior of wooden horizontal hybrid structure Part1(in Japanese), *Journal of structural and construction engineering*, Architectural Institute of Japan, **720**, 291-301